Frost behaviour of a cement structure

A. Fabbri*, T. Fen-Chong, O. Coussy, A. Azouni
Institut Navier, LMSGC (UMR 113 CNRS/LCPC/ENPC), France

Abstract

This study aims at investigating a mechanism that can produce surface scaling of cementitious materials under freezing and thawing without deicing salts. The model allows coupling the liquid/ice crystal thermodynamic equilibrium, Darcean water transport, thermal conduction and thermoelastic properties of the different phases that form the porous material. It predicts that the maximum pore overpressure is reached near the surface, which can result in scaling. Then, the relative influences of the physical processes that produce frost defacement are investigated and the Powers' hydraulic pressure is found to be the most prejudicial one. Finally, macroscopic liquid water transport through the structure is numerically studied, which leads to identify the permeability as a durability indicator towards frost surface damage.

1. Introduction

Frost defacement of civil engineering structures costs millions of euros to cold regions every year. Two kinds of deteriorations are observed: (i) internal frost that takes place within the whole medium and acts as micro-scale damage; (ii) frost scaling that produces the local stick out of surface pieces down to a depth of some millimetres (Marchand *et al.*, 1994).

At a temperature below the bulk freezing point, confined water can partially remain liquid provided that it depressurizes with regard to the adjacent ice crystal (Scherer, 1993). As an initially water-saturated porous material remains filled by both ice and liquid water down to at least $-4\ 0^0\mathrm{C}$, the mechanical response of a porous material results from the combination of the liquid-to-solid expansion and the transport of unfrozen liquid water through the porous network. A poromechanics-based approach that takes account of the thermoelastic behaviour of all phases, has already been worked out to understand and quantify the phenomena both at the pore scale (Coussy and Fen-Chong, 2005) and at the material scale (Coussy, 2005).

This study aims at extending the poromechanics-based approach to the structure scale in order to analyse the relative influences of the physical

* New address : Laboratoire de Géologie de l'Ecole Normale Supérieure

processes that produce frost defacement and the role of the liquid water transport phenomenon on frost scaling behaviour of a cement structure.

2. Poromechanics of a freezing medium

2.1. Water and ice equilibrium

The liquid water (index l) and ice crystal (index c) constitutive equations read in the form:

$$\mathrm{d}\left(\frac{1}{\rho_j}\right) = a_j \mathrm{d}T - \frac{1}{K_j}\mathrm{d}p_j \quad ; \quad \mathrm{d}s = \frac{c_j}{T}\mathrm{d}T - a_j \mathrm{d}p_j \tag{1}$$

where K_j, a_j, and c_j stand for the isothermal bulk modulus, the volumetric thermal dilation coefficient and the heat capacity per mass unit of the phase j while ρ_j, p_j, and s_j are respectively its mass density, pressure, and mass entropy (Coussy, 2004).
The thermodynamic equilibrium between water and ice requires the equality of their specific chemical potentials. Its differentiation, combined with (1), and considering a small density difference between liquid water and ice, furnishes (Fabbri et al., 2006a):

$$p_c = S_f (T - T_0) + C_f \left(T - T_0 + T \ln \frac{T_0}{T}\right) \tag{2}$$

where $S_f = \rho_c^0 \left(s_l^0 - s_c^0\right)$ and $C_f = \rho_c^0 \left(c_{p,l}^0 - c_{p,c}^0\right)$ are respectively the entropy of fusion and the heat capacity differences between water and ice per unit of crystal volume in the reference state at temperature T_0 while $p_c = p_p - p_l$ stands for the capillary pressure.

2.2. Constitutive equations of the porous specimen

Considering the initial state to be $\underline{\underline{\sigma}}(\underline{x},0) = 0$, $\underline{\underline{\varepsilon}}(\underline{x},0) = 0$, $p_l(\underline{x},0) = p_c(\underline{x},0) = 0$, $j_j(\underline{x},0) = 0$, $S(\underline{x},0) = S_0$, and the properties of the solid matrix to be constant, the constitutive equations of the partially frozen material are (Coussy, 2005; Fabbri et al., 2006b):

$$d\underline{\underline{\sigma}} = K\left(d\varepsilon - \frac{2}{3}G\,d\underline{\underline{e}}\right) + G\,d\underline{\underline{\varepsilon}} - \underline{\underline{b}}\left(\sum_{j=l,c}\left(dp_j - K_j\right) + a\,dT\right)\underline{\underline{1}} \tag{3a}$$

$$d\phi_j = d\left(\frac{1}{N_j}p_l + \frac{1}{N_j}p_c\right) - d\alpha_{f_j}T \quad j = l \text{ or } c \tag{3b}$$

$$d\sigma = d\left(K\varepsilon - \sum_{j=l,c} b_j p_j\right) + C_m \frac{dT}{T} \tag{3c}$$

where $\underline{\underline{\sigma}}$ is the stress tensor, $\underline{\underline{\varepsilon}}$ is the strain tensor, $\varepsilon = tr(\underline{\underline{\varepsilon}})$ is the volumetric dilation, ϕ_j is the variation of the partial porosity related to the phase $j = l, c$; K, G, C_m, and α are respectively the bulk modulus, the shear modulus, the heat capacity, and the thermal volumetric dilation coefficient, of the empty porous medium; b_j and N_{ij} are the generalized Biot coefficients and the generalized Biot coupling moduli while α_{f_j} is the coefficient related to the thermal dilation of the pore volume occupied by the phase j. They depend upon the elastic properties of the solid matrix and the saturations of liquid and ice following the relations (Coussy and Monteiro, 2006):

$$\frac{1}{N_j} + \frac{1}{N_c} = \frac{b_j - \phi_0 S_j}{K}; \quad b_c = b_l = 1 - \frac{K}{K_m}; \quad \alpha_{f_j} = \alpha_j - \alpha_m = (b_j - \phi_0)S_j; \quad b_j = S_j\left(1 - \frac{K}{K_m}\right) \tag{4}$$

K_m is the matrix bulk modulus, S_j the saturation ratio of the phase j, and ϕ_0 the initial porosity.

2.3. Overall mass conservation of water

Due to the temperature gradient along the structure, the pressure field is not uniform and a liquid flow is created. Since the ice flow is negligible, the overall mass conservation of water ($m = m_l + m_c$) under the small deformation assumption and the use of (1-4) leads to the following first order expression:

$$d\left[\rho_l^0 \frac{k(S_l)}{\eta_l(T, p_l)}(-\nabla p_l + \rho_l g) - \rho_l a(d\varepsilon)\right] = -A\frac{\partial p_l}{\partial t} + \frac{\partial}{\partial t}\left[T\sum + \sum_{p_{cap}}\right] \tag{5}$$

where $\underline{w} = \rho_l^0 \frac{k(S_l)}{\eta_l(T, p_l)}(-\nabla p_l + \rho_l g)$ stands for the Darcean relative flow vector of mass fluid, $k(S_l)$ and $\eta_l(T, p_l)$ are respectively the permeability of the porous medium and the viscosity of liquid water. The latter is evaluated from a recent empirical relation (Harry and Woolf, 2004) and $A = \phi_0 S_c(1 - K/K_c) + b\phi_0 + K(b - \phi_0)/K_m + \phi_0/K_l$. The source term of liquid

pressure is divided into three distinct contributions: $\Sigma_{\Delta\rho} = \phi_0 S_c \left(\rho_c^0 / \rho_l^0 - 1 \right)$ results from the ice/water mass density change, $\Sigma_T = \phi_0 \left[\alpha_l - \alpha_c S_c + (\alpha_l - \alpha_c) \right] (T - T_0)$ accounts for the difference in thermal dilation between the matrix and the in-pore constituents, $\overset{\circ}{\Sigma}_{cryo} = S_c \left(\phi_0 / K_c - 1/K_m + (b - \phi_0)(4/(3G)) \ldots 1/K_m \right) \frac{dp_{cap}}{dt}$ is a negative decreasing function of cooling ($1/K_m < 1/K_c$) and accounts for the liquid pressure source due to flows at the microscopic scale which drives liquid water to the already frozen sites in order to meet at any time the liquid-crystal equilibrium condition (cryogenic aspiration).

2.4. Thermal conduction

Following the Fourier's Law, the heat flow can be expressed as $\underline{q} = -\lambda(S_l) \frac{\partial T}{\partial x} \underline{x}$, where $\lambda(S_l)$ is the isotropic thermal conductivity and estimated from each phase conductivity using the (n+1)-phase multi-scale scheme (Hervé, 2002). Under these conditions, the second law of thermodynamics applied to the porous medium for a reversible evolution leads to:

$$\frac{d}{dx}\left(\lambda \frac{\partial T}{\partial x} \underline{x} \right) = \frac{\partial T}{\partial t} \left[\left(C_m + \phi_0 \left(C_p S_l + S_c C_c \right) \right) - T_f \phi_0 \left(S_f + C_f \ln \frac{T}{T_f} \right) \frac{\partial S_c}{\partial T} \right] \qquad (6)$$

where $-T \phi_0 \left(S_f + C_f \ln \frac{T}{T_f} \right) \partial S_c / \partial T$ stands for the ice/water phase change latent heat, $C_p = \rho_l^0 c_{p,l}^0$ for the heat capacity of water per unit of volume, and $C_m + \phi_0 \left(C_p S_l + S_c C_f \right)$ represents the average heat capacity of the porous medium.

3. Numerical results

3.1. Sample description and boundary conditions

The specimen is modelled as an one-dimensional structure made up of an isotropic medium, of length L and lateral surface S, ideally insulated on its bottom and lateral surfaces. The Cartesian coordinate system $(O, \underline{x}, \underline{y}, \underline{z})$ is used, with O the centre of the surface which is submitted to frost action and $\underline{x}$ the symmetry axis from the top to the bottom of the

specimen. At the macroscopic scale the flow of heat and liquid only happens in the direction $\underline{x}$ and no water flux ($\underline{w}$) happens through the $x = L$ surface. The analysis will be made using the elementary volume $d\Omega = S dx$.

The specimen bottom side ($x = L$) is initially at $T_b = 283.15$ K, while its top side ($x = 0$) is at $T_t = 273.25$ K. The permanent state is reached before the beginning of the test. Thus the initial temperature of the sample is $T_0(x) = T_t + (T_b - T_t)\, x / L$. Then at $t = 0$, the $x = 0$ surface is submitted to a progressive decrease of temperature while the $x = L$ surface is held at T_b.

In this study, no external loading is applied to the structure. Thus noting $\partial\Omega$ the external surface of the specimen, $\underline{n_{\partial\Omega}}$ the outward unit vector perpendicular to this surface, the mechanical boundary condition can be expressed as $\underline{\underline{\sigma}} \cdot \underline{n_{\partial\Omega}} = 0$ on $\partial\Omega$.

We assume that an impermeable frost layer is created at the $x = 0$ skin surface. In this case, no flow of water occurs through this surface, and the boundary condition will be $\underline{w} \cdot \underline{n_0} = 0$ if $x = 0$ where $\underline{n_0}$ is the outward unit vector perpendicular to the $x = 0$ surface.

3.2. Numerical calculation

The non-linear system (5-6) is solved using the Newton-Raphson method on a structure discretised according to the finite volume method implicit scheme (Eymard *et al.*, 2000).

Numerical calculations are made for a W/C=0.4 hardened cement paste with an initial permeability of 4.3 10^{-21} m^2 and the relative permeability is estimated through the self-consistent differential scheme (Dormieux and Bourgeois, 2003) because water cannot flow through the ice phase. Predicted temperature, ice saturation, ice pressure and liquid pressure profiles are given on figure 1.

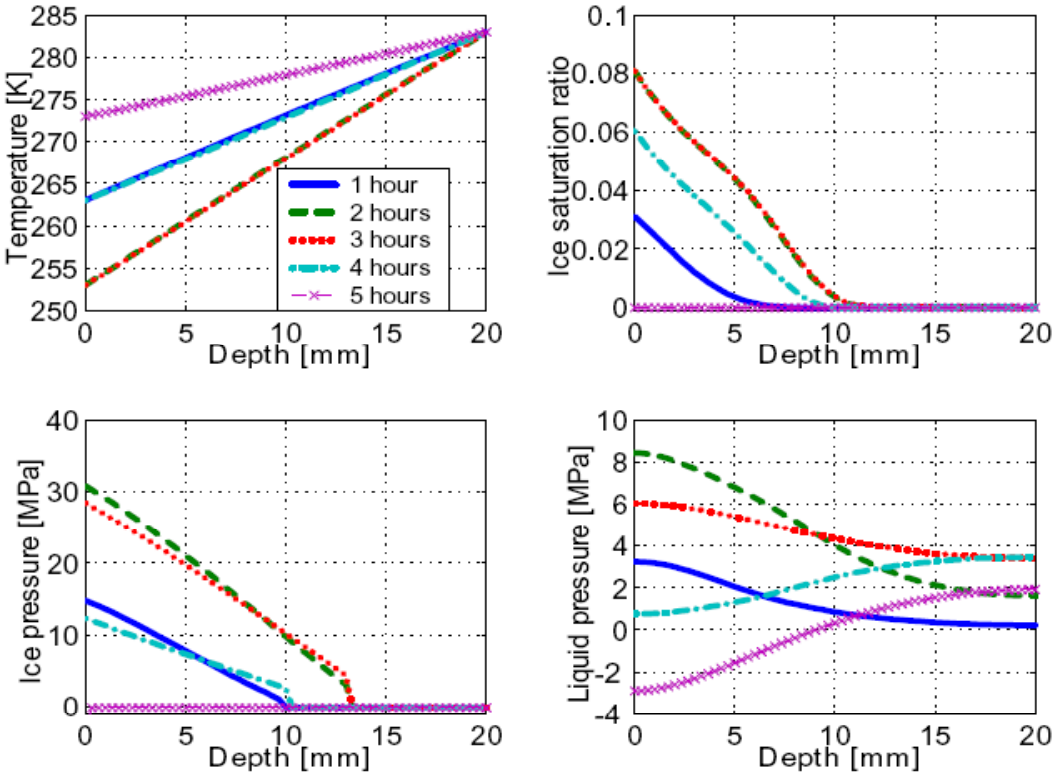

Figure 1: Temperature, ice saturation ratio, ice pressure and liquid pressure predicted from the numerical calculations for a W/C=0.4 hardened cement paste.

As the decrease of temperature penetrates into the specimen, a rise of liquid and ice overpressure and ice saturation ratio, with a maximum near the $x = 0$ surface, is predicted. The higher pressures (30 MPa for ice pressure and 8 MPa for water pressure) are of the same order of magnitude as a W/C=0.4 hardened cement paste tensile strength (round to 10 MPa (Taylor, 1997)). This can explain cement structure scaling submitted to frost action.

The comparison of 1-hour and 4-hour curves shows a hysteresis between the thawing and the freezing behaviours. This is due to the transport of water through the porous network and the hysteresis of the amount of ice. At the end of the thawing stage, liquid water depressurization is predicted near the skin surface. This is the consequence of the water transport from the $x = 0$ surface to the $x = L$ one during the freezing stage combined with the liquid-ice density difference.

4. Physical origin of frost-thaw damages

It is shown in (5) that the frost damage can be attributed to the combination of the hydraulic pressure, the thermal stresses and the cryogenic aspiration. Thanks to the model developed in this study, it is possible to compare the relative importance of these phenomena. The comparison between the pore overpressure profile from a full calculation and calculation without one of the source of liquid pressure terms is reported on figure 2. In order to carry on the comparison, the hydrostatic part of the matrix stress tensor s_m will be studied. As reported in (Coussy, 2004), neglecting the influence of the interfacial tension between liquid water and pore walls, s_m can be linked to the skeleton stress and the equivalent pressures of liquid and crystal by the relation $s_m = \frac{\underline{\underline{s}} - (f_l p_l + f_c p_c)\underline{\underline{1}}}{1 - f_0}$.

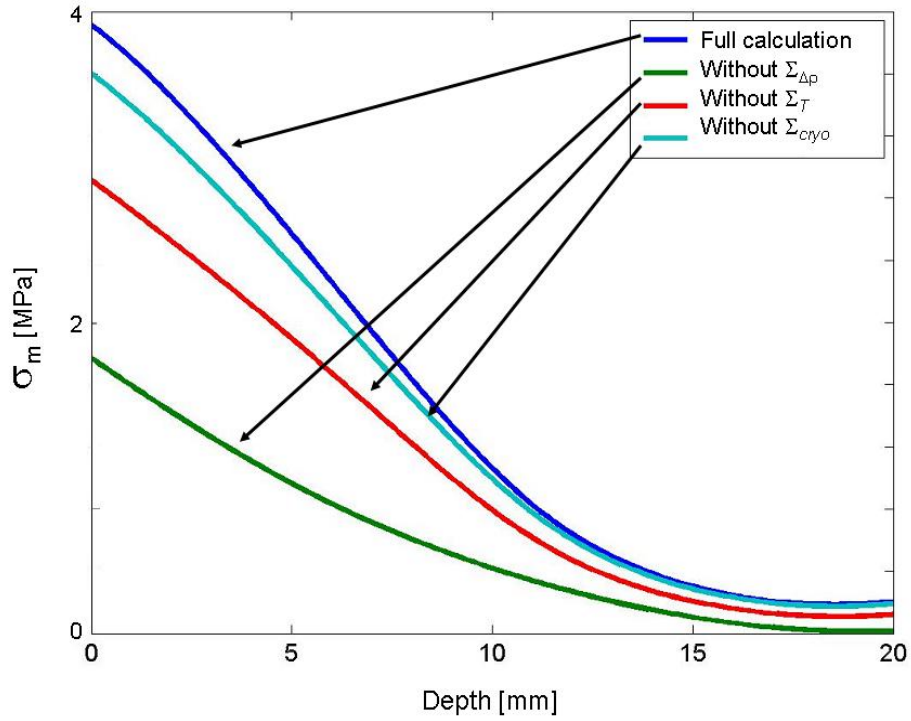

Figure 2: Influence of each source of liquid pressure terms on the s_m profiles.

Let us introduce D*r* as the relative difference on s_m between full and partial calculations. Calculations without Σ_{cryo} leads to D*r*=15%, without

Σ_T leads to D*r*=25% and without $\Sigma_{\Delta r}$ leads to D*r*=55%. In consequence, frost damage appears to be mainly due to the hydraulic pressure. That is why the presence of air void within the material is such efficient to prevent frost damage. Thermal stresses appear also to be important. Finally, the cryogenic aspiration term appears to be a negligible phenomenon from the mechanical standpoint.

Actually, the hydraulic pressure term is such important in case of cementitious material because this type of medium is consolidated, rigid (Young modulus around 50 GPa) and tensile resistant (up to 5-10 MPa). Then, contrary to what is observed in the case of soils frost heave, the overpressure caused by the change-phase volumetric expansion cannot be dissipated by a microstructural modification of the porous network, which results in important matrix stresses.

5. Influence of the permeability

To scan the effect of permeability alone, the predicted matrix hydrostatic stress profiles (at 2 hours) between porous specimens with an initial permeability equal to 4.3×10^{-20} m^2, a ten and a hundred times higher, have been compared.

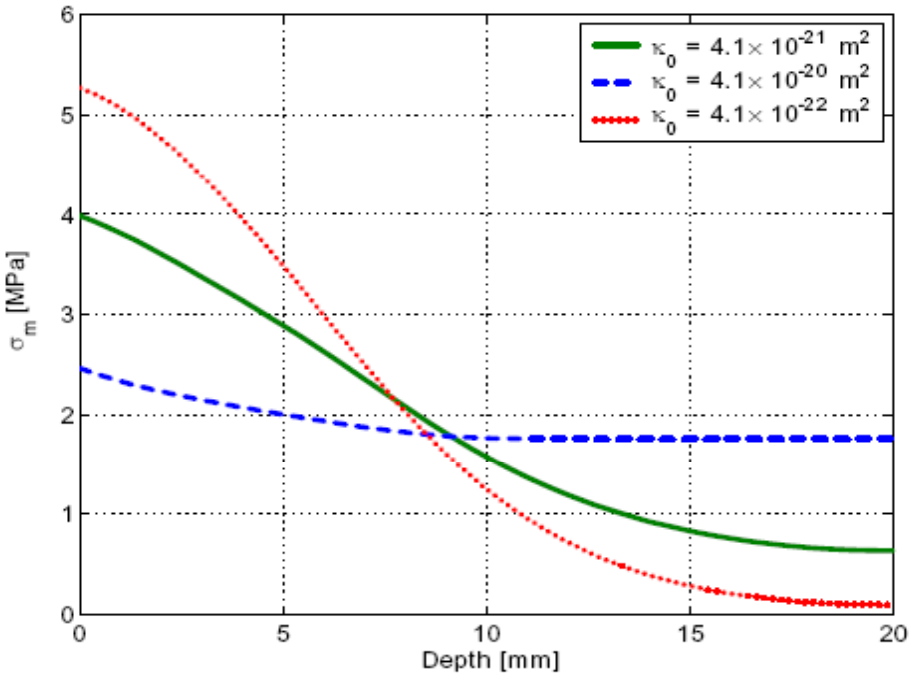

Figure 3: Influence of the permeability on frost-thaw behaviour.

As can be seen on figure 3, when the permeability is increased, the maximum hydrostatic tensile stress in the matrix falls down. It means that a higher permeability allows the liquid water to move easier from the freezing front to the specimen bottom unfrozen part. This explanation is in good agreement with the fact that scaling may be caused by the inability of the frozen porous network to relax local overpressure from the skin surface. In addition, it explains experimental data from (Baroghel-Bouny *et al.,* 2002) where a concrete with a compressive strength equal to 50 MPa exhibit a better frost durability than a less permeable high resistance concrete (with a compressive strength equal to 75 MPa).

So, in case of initial and boundary conditions which force the top surface temperature to be lower than the bottom one, water will first freeze near the skin surface. If the amount of ice formed is important enough and the permeability is too small to relax pore overpressure, scaling will occur. Thus, it appears to be a localised "internal frost"-like damage enhanced by the $x = 0$ surface boundary condition.

6. Conclusion

It is here investigated the frost behaviour of a cementitious structure. The poromechanical-based approach is first used in order to investigate the relative influence of the physical processes that produce frost defacement is investigated. The Powers' hydraulic pressure is found to be the most prejudicial one and the permeability is identified as a durability indicator towards frost surface damage.

Then, the model is used to understand the role of permeability towards frost durability. This study shows that scaling is more likely to happen in low permeable structure. Indeed, in this case , the relaxation of pore overpressure near the surface submitted to frost action is not sufficient to protect the specimen from scaling.

References

V. Baroghel-Bouny, S. Arnaud, D. Henry, M. Carcasses, D. Quenard (2002) Vieillissement des bétons en milieu naturel : une expérimentation pour le XXIe siècle. III - Propriétés de durabilité des bétons mesurées sur éprouvettes conservées en laboratoire. *Bulletin des Laboratoires des Ponts et Chaussées, **241**, 13-59*.

O. Coussy (2004) *Poromechanics.* John Wiley & Sons.

O. Coussy (2005) Poromechanics of freezing materials. *Journal of the Mechanics and Physics of Solids, **53**, 1689-1718*.

O. Coussy, T. Fen-Chong (2005) Crystallization, pore relaxation and micro-cryosuction in cohesive porous materials. *Comptes Rendus Mecanique, **333** (6), 507-512.*

O. Coussy, Paulo J.M. Monteiro (2006) Unsaturated poroelasticity for crystallization in pores. *Cement and Concrete Research*, *submitted.*

L. Dormieux, E. Bourgeois (2003) *Introduction à la micromécanique des milieux poreux*, Presses de l'École Nationale des Ponts et Chaussées.

R. Eymard, T. Gallouet, R. Herbin (2000) Finite Volume Methods, p.723-1020*, Handbook for numerical analysis, Vol. VII, Editors: P.G. Ciarlet and J.L. Lions. North-Holland.*

A. Fabbri, T. Fen-Chong, O. Coussy (2006) Dielectric capacity, liquid water content, and pore structure of thawing-freezing materials. *Cold Regions Science and Technology, **44**, 52-66.*

A. Fabbri, O. Coussy, T. Fen-Chong, P.J.M. Monteiro (2006) Are deicing salts necessary to promote scaling in concrete ? *Journal of Engineering Mechanics, submitted.*

K.R. Harris, L.A. Woolf (2004) Temperature and volume dependence of the viscosity of water and heavy water at low temperatures. *Journal of Chemical and Engineering Data*, ***49** (4), 1064-1069.*

E. Hervé (2002) Thermal and thermoelastic behaviour of multiply coated inclusion-reinforced composites. *International Journal of Solids and Structures, **39**, 1041-1058.*

J. Marchand, E.J. Sellevold, M. Pigeon (1994) The deicer salt scaling deterioration of concrete - an overview. In V.M. Malhotra, editor, *Durability of concrete. Proceedings of third CAMNET-ACI International Conference, Nice.*

G.W. Scherer (1993) Freezing gels, *Journal of Non Crystalline Solids*, ***155**, 1-25.*

H.F.W. Taylor (1997) *Cement Chemistry - 2nd Edition*. *Thomas Telford Publishing.*